

# CHEMISTRY

## A European Journal

A Journal of



### Accepted Article

**Title:** Pyrimidopteridine N-Oxide Organic Photoredox Catalysts: Characterization, Application and Non-Covalent Interaction in Solid State

**Authors:** Richy Hauptmann, Andranik Petrosyan, Franziska Fennel, Miguel André Argüello Cordero, Annette-Enrica Surkus, and Jola Pospech

This manuscript has been accepted after peer review and appears as an Accepted Article online prior to editing, proofing, and formal publication of the final Version of Record (VoR). This work is currently citable by using the Digital Object Identifier (DOI) given below. The VoR will be published online in Early View as soon as possible and may be different to this Accepted Article as a result of editing. Readers should obtain the VoR from the journal website shown below when it is published to ensure accuracy of information. The authors are responsible for the content of this Accepted Article.

**To be cited as:** *Chem. Eur. J.* 10.1002/chem.201900118

**Link to VoR:** <http://dx.doi.org/10.1002/chem.201900118>

Supported by  
**ACES**

WILEY-VCH

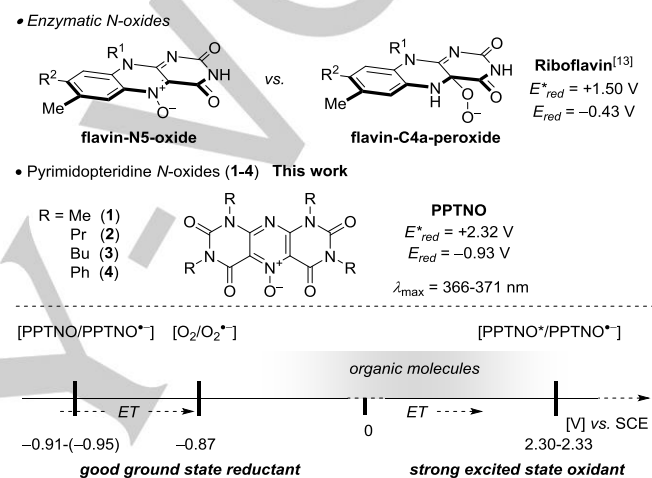
# Pyrimidopteridine *N*-Oxide Organic Photoredox Catalysts: Characterization, Application and Non-Covalent Interaction in Solid State

Richy Hauptmann<sup>†</sup>,<sup>[a]</sup> Andranik Petrosyan<sup>†</sup>,<sup>[a]</sup> Franziska Fennel,<sup>[b]</sup> Miguel A. Argüello Cordero,<sup>[a,b]</sup> Annette-E. Surkus,<sup>[a]</sup> and Jola Pospech<sup>\*[a]</sup>

**Abstract:** Herein we report the photo- and electrochemical characterization of pyrimidopteridine *N*-oxide based heterocycles. The potential of their application as organic photoredox catalyst is showcased in the photomediated contra-thermodynamic  $E \rightarrow Z$  isomerization of cinnamic acid derivatives and oxidative cyclization of 2-phenyl benzoic acid to benzocoumarin using molecular oxygen as a mild oxidant. Furthermore, unprecedented intermolecular non-covalent  $n-\pi$  hole interactions in solid state are discussed based on crystallographic and theoretic data.

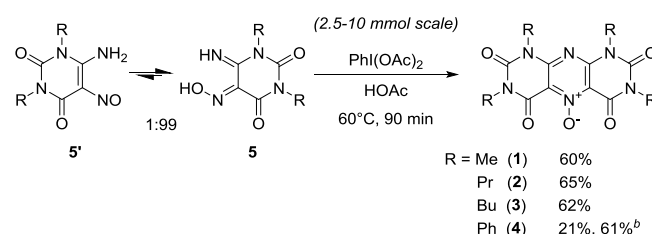
Recently there has been convincing evidence that flavin-*N5*-oxide serves as a viable intermediate in enzyme-catalyzed oxygenation reactions besides the well-established flavin-*C4a*-peroxide.<sup>[1]</sup> Based on spectroscopic and spectrometric studies, the stable flavin-*N5*-oxide has been postulated to participate in reactions involving EncM monooxygenase, provoking oxidative carbon rearrangement,<sup>[2]</sup> dibenzothiophene catabolism<sup>[3]</sup> and oxidative cleavage of uracil amides.<sup>[4]</sup> However, till date the actual catalytic potential of flavin-*N5*-oxides remains largely unexplored.<sup>[5]</sup> The structurally related 1,3,7,9-tetra-butyl-2,4,6,8-tetraoxo-[5,4-*g*]pteridine 5-oxide (BuPPT *N*-oxide, **3**) has first been reported by the group of Maki in 1986 and has been applied in various photo-mediated oxygen atom transfer reactions leading to *N*-demethylation,<sup>[6]</sup> C-H oxygenation<sup>[7]</sup> and oxidative C-C bond scission reactions<sup>[8]</sup> as a stoichiometric oxygen atom transfer reagent. Since the initial reports, no further investigation concerning its photoredox properties and applicability in catalytic reactions has been attempted. In view of the latest findings in flavin chemistry, these structures may serve as an important link between organic photoredox catalysis and chemical biology. We have optimized the synthesis of 4 different PPTNO photosensitizers on gram-scale. Besides the previously reported BuPPT *N*-oxide (**3**), we prepared its tetramethyl (MePPT *N*-oxide, **1**), tetrapropyl (PrPPT *N*-oxide, **2**), and tetraphenyl (PhPPT *N*-oxide, **4**) derivatives via modified procedure.<sup>[9]</sup> Photo- and electrochemical analysis revealed that all compounds have large excited state energies, and are capable of oxidizing compounds with oxidation potentials exceeding +2.0 V. Furthermore, the radical anions resulting from photoinduced electron transfer are moderate to good reductants, and turnover with mild oxidants such as dioxygen. The heteroarene based photosensitizers display excellent stability

and robustness as compared to commonly used photosensitizers. In addition, the solid state analysis of *N*-oxides **1-4** reveal interesting non-covalent intermolecular interactions that are indicative of lone-pair- $\pi$ -hole interaction based on crystallographic and theoretic data.



**Scheme 1.** Structural, electro- and photochemical properties of photosensitizers **1-4**.

The synthesis of the pyrimidopteridine *N*-oxides **1-3** was accomplished by radical dimerization of the corresponding 6-amino-5-nitrosouracils (**5'**), which according to spectroscopic data is better described as 5-hydroimino-6-imino tautomer **5**. The dimerization is provoked by phenyliodine(III) diacetate (PIDA) and the desired condensed heterocycles were isolated in 60-65% yield on gram-scale by recrystallization. The phenyl derivative **4** was obtained in significantly higher yield when lead tetraacetate was used as oxidant.<sup>[10]</sup>



**Scheme 2.** Synthesis of PPT *N*-oxides **1-4**. [a] All yields are isolated yields purified by crystallization. [b] Pb(OAc)<sub>4</sub> was used instead of PhI(OAc)<sub>2</sub>.

[a] M.Sc. R. Hauptmann, Dipl.-Chem. A. Petrosyan, M.Sc. M. A. Argüello Cordero, Dr. A.-E. Surkus, Dr. J. Pospech  
 Leibniz Institute for Catalysis at University of Rostock, Department  
 Albert-Einstein-Strasse 29a, D-18059 Rostock, Germany.  
 E-mail: Jola.Pospech@catalysis.de

[b] Dr. F. Fennel, M.Sc. M. A. Argüello Cordero  
 Department of Physics, Rostock University, Albert-Einstein-Str.  
 23-24, 18059 Rostock, Germany.

† These authors contributed equally

**Table 1.** Photophysical and Electrochemical Properties of PPTNO Photosensitizers.

compound	$\lambda_{max}^{abs}$ [nm]	$\phi_f$	excited state energy $E_{0,0}^{S1a}$ [eV]	ground state redox potentials (V vs SCE)		excited state redox potentials (V vs SCE)	
				$E_{1/2}^{red}$	$E_{1/2}^{ox}$	$E_{red}^*$	$E_{ox}^*$
1	368	0.69	+3.24	-0.91	+2.42	+2.33	-0.82
2	370	1.86	+3.25	-0.95	+2.42	+2.30	-0.83
3	371	0.40	+3.25	-0.92	+2.47	+2.33	-0.78
4	366	0.24	+3.25	-0.93	+2.33	+2.32	-0.92

[a]  $E_{0,0}$  values corresponding to the energy at the intersection of the excitation and emission spectra. [b] Potentials were measured using cyclic voltammetry (CV) and differential pulse voltammetry (DPV) relative to  $Fc^+/Fc$ ; referenced to SCE by adding 0.42 V to the value relative to  $Fc^+/Fc$ .<sup>[11]</sup> [c] Calculated by  $E_{red}^{S1} = E_{0,0}^{S1} + E_{red}^{1/2}$ . [d] Calculated by  $E_{ox}^{S1} = E_{ox}^{1/2} - E_{0,0}^{S1}$ .

transitions, respectively. The aromatic  $\pi \rightarrow \pi^*$  transition in the phenyl derivative are visible but structureless. The emission spectra of *N*-alkyl substituted derivatives **1–3** show an emission maximum at 398 nm resulting in a Stokes shift of approximately 30 nm (0.25 eV). The emission spectra of **1**, **2** and **3** exhibited close to mirror-image symmetry and the quantum yields are between 0.4% and 1.86%. In contrast, the emission spectra of phenyl-bearing **4** had a broad shape with a maximum at 423 nm, indicative of an enhanced charge transfer character in the excited state in the presence of aryl substituents on the pyrimido pteridine core. The strong charge transfer character of the excited state is supported by the further reduced quantum yield of 0.23%. Nevertheless,  $E_{0,0}$  values corresponding to the energy at the intersection of the absorption and emission spectra and were close to unity for all PPTNOs **1–4** at 382 (1) nm (3.25 eV) and are listed in Table 1. Cyclic voltammetry (CV) was employed to determine the ground state redox potentials ( $E_{ox}$  and  $E_{red}$ ) of compounds **1–4**. All compounds exhibit an irreversible anodic oxidation at potentials above +2.20 V. The heteroarene *N*-oxides **1–4** experience two consecutive reductions around -0.93 V and -1.20 V which could not be separated from one another. As a consequence, the re-oxidation peaks were ill-defined which compromises the correct determination of the half-wave potential. This is a common problem in electrochemical measurements. Figure 2 shows the differential pulse voltammograms (DPV) of the reduction and oxidation waves of the pyrimidopteridine *N*-oxides against the  $Fc^+/Fc$  redox couple. The diagrams show the measurements of the cathodic reduction (left) and anodic oxidation (right). DPV uses a series of voltage pulses superimposed on the linear sweep potential and the current change is plotted against the potential. The signal maximum is a good approximation of the half wave potential  $E_{1/2}$  and can be determined without the prerequisite of showing defined peaks for the anodic and cathodic current as required in CV measurements and thus allows a more facile determination of redox potentials. The potentials listed in Table 1 were referenced to SCE by adding 0.42 V to the value relative to  $Fc^+/Fc$ .<sup>[11]</sup> The excited state potentials  $E_{red}^*$  and  $E_{ox}^*$  were determined by employing optical and electrochemical data. The

high excited state energies of +3.25 V for **1–4** turn the compounds into very potent excited state oxidants with excited state reduction potentials of +2.30 V and higher. Thus, the *N*-oxides **1–4** are well-suited for the activation of a great number of substrates in their excited state. At the same time, the reduced  $PPTNO^{\cdot-}$  [ $E_{1/2}^{red}(PPTNO/PPTNO^{\cdot-}) = -0.91$  eV for **1** vs SCE in MeCN] are oxidized by mild oxidants, such as molecular oxygen [ $E_{1/2}^{red}(O_2/O_2^{\cdot-}) = -0.87$  eV vs SCE in MeCN].<sup>[12]</sup> In comparison, the reduction potential of riboflavin is -0.43 V with an excited state reduction potential of +1.50 V (vs SCE in water).<sup>[13]</sup> Overall, the photo- and electrochemical properties render the studied compounds excellent candidates for applications in organic photoredox catalysis.

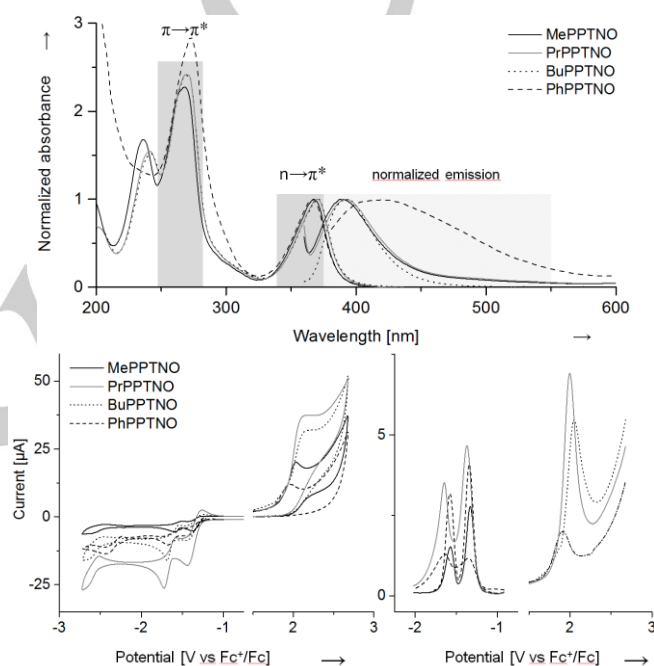
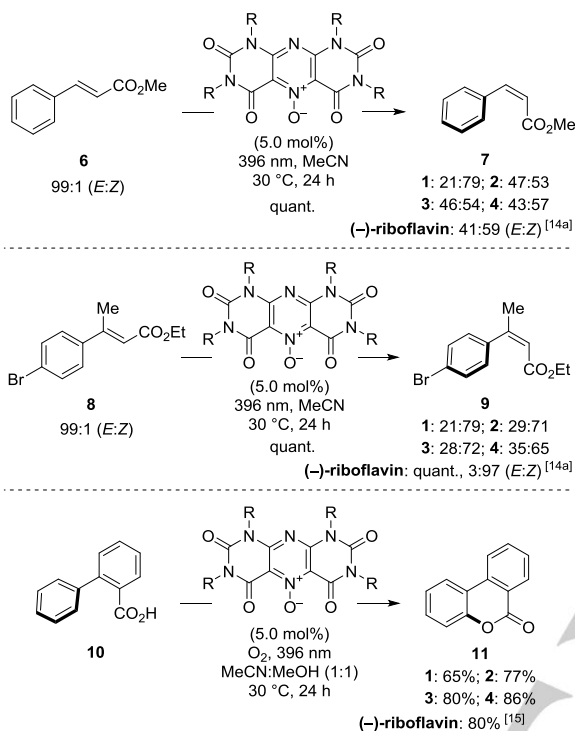


**Figure 2.** UV-vis absorption and emission spectra (top); Cyclic voltammogram (CV) (bottom left); Differential pulse voltammograms (DPV) of PPTNOs **1–4** against the  $Fc^+/Fc$  redox couple.

Herein, we showcase the catalytic activity of the synthesized pyrimidopteridine *N*-oxides in representative reactions that have previously been reported using (-)-riboflavin as organic photoredox catalyst. For instance, the PPTNO photocatalyst demonstrate a similar behavior as compared to the (-)-riboflavin-based system by inducing a contra-thermodynamic  $E \rightarrow Z$  isomerization of cinnamic acid derivatives via productive energy transfer ( $E_T$ ).<sup>[14],[15]</sup> Methyl cinnamate (**6**) was isomerized to a mixture of *E*- and *Z*-methyl cinnamate (**7**) in a 43:57 ratio using phenyl derivative **4**. In comparison, (-)-riboflavin promoted the same reaction in a 41:59 isomeric ratio. The isomerization of *E* to *Z* ethyl 3-(4-bromophenyl)but-2-enoate (**8**) proceeds in lower selectivity of a maximum of 21:79 (*E*:*Z*) using MePPTNO (**1**) as compared to riboflavin system but still exemplifies the proof of concept. To our delight, a cyclization of [1,1'-biphenyl]-2-carboxylic acid (**10**) to benzocoumarin **11** was accomplished in 86% isolated yield under unoptimized reaction conditions.

Noteworthy, the (–)-riboflavin-based system suffers from catalyst degradation in course of the SET reaction, necessitating the iterative addition of catalyst in batches of 5.0 mol% every 12 hours.<sup>[16]</sup> The experiments presented herein, were conducted on a 0.5 mmol scale using only a single batch of 5.0 mol% of the organocatalyst.



**Scheme 1.** Photo-mediated *E/Z*-isomerization and benzocoumarin synthesis.

The pyrimidopteridine heterocycles can be stored under ambient conditions, without any signs of degradation as crystalline material.<sup>[17]</sup> Crystals suitable for single crystal analysis were obtained for the *N*-oxide derivatives **1–4**. The PPTNOs showed interesting non-covalent interactions. The view perpendicular (A) and along (B) the heteroarene plane is depicted in Figure 2. The molecules are arranged in a stair-like fashion in which the *N*-oxide oxygen atom interacts with the heteroarene core of the adjacent molecule. This interaction is most pronounced in the propyl and methyl derivatives **1** and **2**, resulting in a near perpendicular arrangement of the single molecules in the crystal package of 85° and 76°, respectively between the planes defined by the C(4a)–N(5)–C(5a) plane of two neighboring molecules (Table 2). The more bulky butyl substituents tame the interaction. The neighboring molecules of **3** are tilted in an angle of 29°. However, in each case, the *N*-oxide oxygen and pyrimidine core are in close contact of a mean value of 2.76 Å. The intramolecular interactions in the solid state are reminiscent of lone-pair– $\pi$  hole or anion– $\pi$  hole interactions that are often apparent between electron-rich species and electron-deficient arenes.<sup>[18]</sup> Such non-covalent interactions (NCI) have recently attracted much attention particularly regarding ion transport in biomolecular structures and catalysis.<sup>[19],[20]</sup> In order to clarify the origin of the molecular arrangement in the crystal structure, we

applied DFT calculations for MePPTNO (**1**) on a B3LYP/6-31G(d,p) level of theory.<sup>[21]</sup> The differences in the charge distributions within the molecule were visualized by an electrostatic potential (ESP) map depicted in Figure 3. The red color represents an excess of electron density and electron-deficient regions are colored in blue. Accordingly, the electron density accumulates at the carbonyl–*N*-oxide–carbonyl portion of the molecule whereas the center of the aromatic rings are

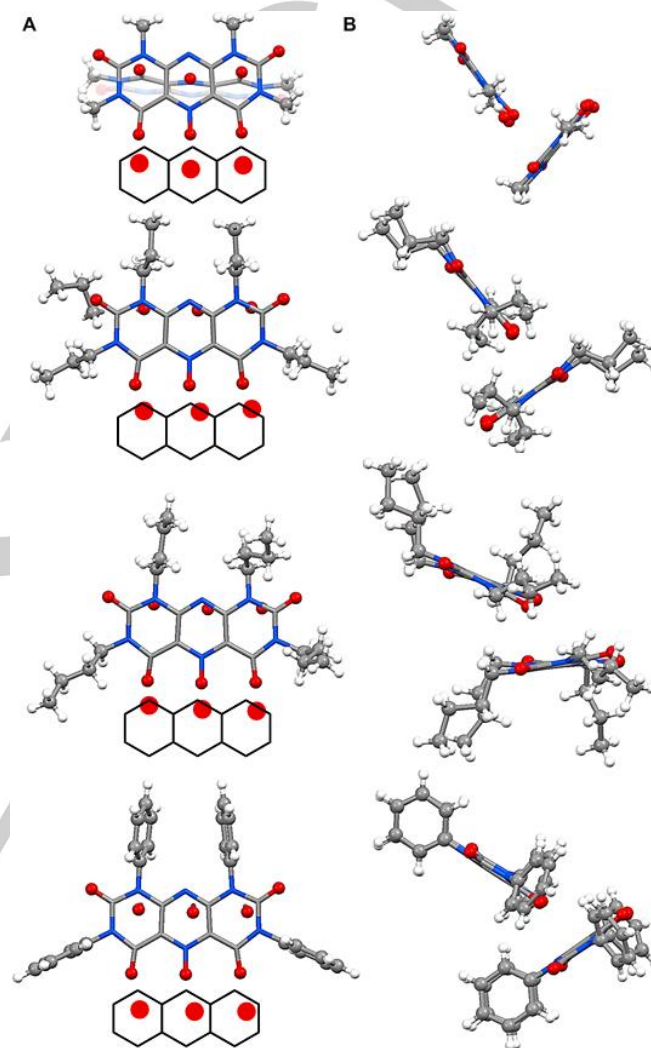


**Figure 3.** Crystal structures of PPTNOs **1–4** in (A) top and (B) side view.

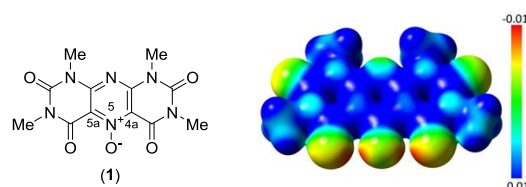


**Figure 4.** Electrostatic potential map of MePPTNO (**1**) showing electron-rich (red) and electron-poor regions (blue).

electron deprived regions and are thus well suited for anion or lone-pair interaction.

In the pyrimidopteridines *N*-oxides, the *d*(N–O) bond lengths are relatively short, with a mean value of about 1.26 Å. In comparison with typical N–O single bonds in hydroxylamines (1.45 Å) and N=O double bonds in nitrosoalkanes (1.27 Å), the crystallographic data suggests that this bond should be considered as a strong non-polar dative N–O bond, stabilized by  $\pi$ -type N–O back-donation, rather than a polar covalent bond N<sup>+</sup>–O<sup>-</sup>.<sup>[22]</sup> Thus, we propose that the NCI originates from lone-pair– $\pi$ -hole rather than anion– $\pi$ -hole interaction.

**Table 2.** *N*-Oxide N–O bond length; distance of lone-pair– $\pi$  hole interaction and angles between two adjacent molecules.

compounds	<i>d</i> (N–O) [Å]	<i>d</i> (O–pyr) [Å] <sup>[a]</sup>	angle <sup>[b]</sup>
1	1.257	2.719	76°
2	1.256	2.797	85°
3	1.263	2.783	29°
4	1.257	2.765	68°

[a] Distance between O(5) atom and plane defined by C(4a)–N(5)–C(5a); [b] angle between two planes defined by C(4a)–N(5)–C(5a) of neighbouring molecules.

In summary, we report the photo- and electrochemical characterization of pyrimidopteridine *N*-oxide based heterocycles. The heteroarene based photosensitizers display excellent stability and robustness as compared to commonly used photosensitizers and can be synthesized on gram-scale from inexpensive starting material. Here, we demonstrated its application as potent organic photoredox catalyst for the first time. Furthermore, unprecedented intermolecular non-covalent  $n$ – $\pi$  hole interactions of the pyrimidopteridine *N*-oxides based on crystallographic data is described and is supported by DFT calculations.

## Acknowledgements

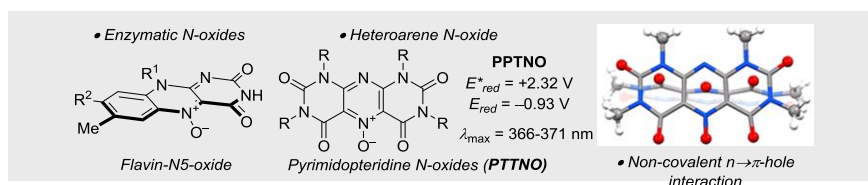
This work was funded by the Deutsche Forschungsgemeinschaft (DFG, German Research Foundation) – 401007518 and by the European Union (ESF/14-BM-A55-0049/16). We thank Dr. Anke Spannenberg (LIKAT) and Dr. Alexander Villinger (Rostock University) for crystallographic measurements and Dr. Nils Rockstroh for assistance with the measurements of emission spectra. Moreover, we would like to express our gratitude to the LIKAT for excellent support.

**Keywords:** Organo Photoredox Catalysis • Non-Covalent Interactions • Heteroarene *N*-oxides • Heterocycles

- [1] a) E. Romero, J. R. Gómez Castellanos, G. Gadda, M. W. Fraaije, A. Mattevi, *Chem. Rev.* **2018**, *118*, 1742-1769; b) R. Teufel, V. Agarwal, B. S. Moore, *Curr. Opin. Chem. Biol.* **2016**, *31*, 31-39; c) R. Teufel, *Arch. Biochem. Biophys.* **2017**, *632*, 20-27; d) V. Piano, B. A. Palfey, A. Mattevi, *Trends Biochem. Sci.* **2017**, *42*, 457-469.
- [2] a) R. Teufel, F. Stull, M. J. Meehan, Q. Michaudel, P. C. Dorrestein, B. Palfey, B. S. Moore, *J. Am. Chem. Soc.* **2015**, *137*, 8078-8085; b) R. Teufel, A. Miyanaga, Q. Michaudel, F. Stull, G. Louie, J. P. Noel, P. S. Baran, B. Palfey, B. S. Moore, *Nature* **2013**, *503*, 552.
- [3] S. Adak, T. P. Begley, *J. Am. Chem. Soc.* **2016**, *138*, 6424-6426.
- [4] S. Adak, T. P. Begley, *Biochemistry* **2017**, *56*, 3708-3709.
- [5] a) T. Hering, B. Mühldorf, R. Wolf, B. König, *Angew. Chem. Int. Ed.* **2016**, *55*, 5342-5345; b) C. Feldmeier, H. Bartling, K. Magerl, R. M. Gschwind, *Angew. Chem. Int. Ed.* **2015**, *54*, 1347-1351.
- [6] M. Sako, K. Shimada, K. Hirota, Y. Maki, *J. Am. Chem. Soc.* **1986**, *108*, 6039-6041.
- [7] a) M. Sako, S. Ohara, K. Hirota, Y. Maki, *J. Chem. Soc. Perkin Trans 1* **1990**, 3339-3344; b) M. Sako, K. Hirota, Y. Maki, *Chem. Pharm. Bull.* **1990**, *38*, 2069-2071; c) M. Sako, S. Ohara, K. Shimada, K. Hirota, Y. Maki, *J. Chem. Soc. Perkin Trans 1* **1990**, 863-868.
- [8] a) M. Sako, K. Shimada, K. Hirota, Y. Maki, *Tetrahedron Lett.* **1986**, *27*, 3877-3880; b) Y. Maki, M. Sako, I. Oyabu, T. Murase, Y. Kitade, K. Hirota, *J. Chem. Soc. Chem. Commun.* **1989**, 1780-1782; c) Y. Maki, I. Oyabu, S. Ohara, M. Sako, Y. Kitade, K. Hirota, *Chem. Pharm. Bull.* **1989**, *37*, 3239-3242.
- [9] The synthesis involves a radical dimerization of a nitrosoamino intermediate. In the seminal report, this step was accomplished using lead(IV) tetraacetate. We have successfully revised this sequence using phenyliodo diacetate (PIDA) as radical initiator.
- [10] A detailed comparison on the performance of PhI(OAc)<sub>2</sub> vs Pb(OAc)<sub>4</sub> is reported in the SI.
- [11] H. G. Roth, N. A. Romero, D. A. Nicewicz, *Synlett* **2016**, *27*, 714-723.
- [12] D. T. Sawyer, G. Chiericato, C. T. Angelis, E. J. Nanni, T. Tsuchiya, *Anal. Chem.* **1982**, *54*, 1720-1724.
- [13] C. Lu, W. Lin, W. Wang, Z. Han, S. Yao, N. Lin, *Phys. Chem. Chem. Phys.* **2000**, *2*, 329-334.
- [14] a) J. B. Metternich, R. Gilmour, *J. Am. Chem. Soc.* **2015**, *137*, 11254-11257; b) J. J. Molloy, J. B. Metternich, C. G. Daniliuc, A. J. B. Watson, R. Gilmour, *Angew. Chem.* **2018**, *130*, 3222-3226; c) J. B. Metternich, D. G. Artiukhin, M. C. Holland, M. von Bremen-Kühne, J. Neugebauer, R. Gilmour, *J. Org. Chem.* **2017**, *82*, 9955-9977; d) J. B. Metternich, R. Gilmour, *Synlett* **2016**, *27*, 2541-2552.
- [15] For an example using a fluorene catalyst, see: W. Cai, H. Fan, D. Ding, Y. Zhang, W. Wang, *Chem. Commun.* **2017**, *53*, 12918-12912.
- [16] a) J. B. Metternich, R. Gilmour, *J. Am. Chem. Soc.* **2016**, *138*, 1040-1045; b) T. Morack, J. B. Metternich, R. Gilmour, *Org. Lett.* **2018**, *20*, 1316-1319.
- [17] All compounds can be stored for >1 year without any evidence of physical changes or alteration of their photochemical properties.
- [18] S. K. Singh, A. Das, *Phys. Chem. Chem. Phys.* **2015**, *17*, 9596-9612.
- [19] A. J. Neel, M. J. Hilton, M. S. Sigman, F. D. Toste, *Nature* **2017**, *543*, 637.
- [20] M. Giese, M. Albrecht, K. Rissanen, *Chem. Commun.* **2016**, *52*, 1778-1795.
- [21] For detailed information, see S53.
- [22] M. Łukomska, A. J. Rybarczyk-Pirek, M. Jabłoński, M. Palusiak, *Phys. Chem. Chem. Phys.* **2015**, *17*, 16375-16387.

## Entry for the Table of Contents

## COMMUNICATION



Richy Hauptmann, Andranik Petrosyan,  
 Franziska Fennel, Miguel A. Argüello  
 Cordero, Annette-Enrica Surkus, Jola  
 Pospech\*

Page No. – Page No.

**Pyrimidopteridine *N*-Oxide Organic  
 Photoredox Catalysts:  
 Characterization, Application and  
 Non-Covalent Interaction in Solid  
 State**

Pyrimidopteridine *N*-oxide based heterocycles exhibit excellent excited state reduction potentials paired with a suitable ground state reduction potential allowing for catalyst turnover with mild oxidants. The structural similarity between pyrimidopteridines and recently uncovered flavine *N*-oxides may draw an important link between organic photoredox catalysis and chemical biology.